Journal of ELECTRONIC MATERIALS, Vol. 45, No. 1, 2016
DOI: 10.1007/s11664-015-4107-8

Recent Progress in Ohmic Contacts to Silicon Carbide for High-Temperature Applications

ZHONGTAO WANG,[1] WEI LIU,[1] and CHUNQING WANG[1,2,3]

1.—State Key Laboratory of Advanced Welding and Joining, Harbin Institute of Technology, Harbin 150001, China. 2.—Electronics Packaging Group, School of Materials Science and Engineering, Harbin Institute of Technology, Harbin 150001, China. 3.—e-mail: wangcq@hit.edu.cn

During the past few decades, silicon carbide (SiC) has emerged as the most promising wide-bandgap semiconductor for high-temperature, high-frequency, and high-power applications. All its attractive properties depend critically on and are often limited by the formation of Ohmic contacts to SiC. Although impressive progress has been made, improvements to further reduce the specific contact resistance without lowering the stability of Ohmic contacts during long-term aging are still indispensable. In this regard, we present a review of recent progress in Ohmic contacts to *n*- and *p*-type SiC reported in literature. The mechanism of Ohmic contact to SiC, surface preparation methods, and performance of Ohmic contacts are discussed. Emphasis is placed on the thermal stability of Ohmic contacts to SiC. To date, extremely low specific contact resistance values (10^{-7} Ω cm^2 to 10^{-6} Ω cm^2) have been obtained after high-temperature (>800°C) annealing. Moreover, great efforts have been made to achieve good Ohmic contact performance (10^{-6} Ω cm^2 to 10^{-5} Ω cm^2) under low-temperature annealing (<600°C) or even without annealing. During long-term aging at high temperature (300°C to 1000°C), surface morphology degradation, formation of unwanted Kirkendall voids, interdiffusion between metallization stacks and/or SiC substrates, and especially severe oxidation in oxygen-containing atmospheres can be responsible for electrical degradation of Ohmic contacts. These critical issues are discussed along with future perspectives.

Key words: Silicon carbide, Ohmic contacts, thermal stability, high temperature, wide-bandgap semiconductors

INTRODUCTION

SiC has many promising characteristics such as high breakdown voltage, high thermal conductivity, high saturation electron drift velocity, and good chemical stability, as summarized in Table I,[1,2] which are attractive for fabrication of devices used in high-temperature, high-frequency, and high-power applications in place of Si-based devices.[3,4] However, application of SiC as a semiconductor is hampered by difficulties in controlling metal/SiC contact properties in SiC-based electronic devices including bipolar junction transistors (BJTs),[5–7] junction field-effect transistors (JFETs),[8,9] metal–semiconductor field-effect transistors (MESFETs),[10,11] metal–oxide–semiconductor field-effect transistors (MOSFETs),[12,13] insulated gate bipolar transistors (IGBTs),[14,15] etc. Degradation of metal/SiC contacts, or relatively high specific contact resistance between metal and SiC, may cause an inadmissible voltage drop at metal/SiC contacts, hampering application of high-temperature or high-power SiC devices[16–21] such as power MOSFETs.[22–24] Degradation of metal/SiC contacts is due to reactions of metal with SiC and/or interdiffusion of metal stacks, followed by formation of silicides, carbides, and oxides plus free carbon generation during long-time and high-temperature operation in air or harsh environments. Thus, Ohmic contact structures

(Received April 14, 2015; accepted September 30, 2015; published online November 3, 2015)

Table I. Major physical properties of 3C-, 4H-, and 6H-SiC

Physical Property/SiC Polytype		3C-SiC	4H-SiC	6H-SiC
Lattice constant				
a	(Å)	4.3596	3.0798	3.0805
c	(Å)	–	10.0820	15.1151
Bandgap	(eV)	2.36	3.26	3.02
Electron affinity	(eV)	4.0	3.8	3.3
Electron effective mass				
$m_{\parallel}(m_0)$	–	0.67	0.33	2.0
$m_{\perp}(m_0)$	–	0.25	0.42	0.48
Hole effective mass				
$m_{\parallel}(m_0)$	–	~1.5	1.75	1.85
$m_{\perp}(m_0)$	–	~0.6	0.66	0.66
Effective density of states in the conduction band	($\times 10^{19}$ cm^{-3})	1.5	1.8	8.8
Effective density of states in the valence band	($\times 10^{19}$ cm^{-3})	1.9	2.1	2.2
Electron mobility at low doping				
$\mu_{\parallel}(c-\text{axis})$	(cm^2 V^{-1} s^{-1})	~1000	1200	100
$\mu_{\perp}(c-\text{axis})$	(cm^2 V^{-1} s^{-1})	~1000	1020	450
Hole mobility at low doping	(cm^2 V^{-1} s^{-1})	100	120	100
Electron saturated drift velocity	($\times 10^7$ cm s^{-1})	~2	2.2	1.9
Hole saturated drift velocity	($\times 10^7$ cm s^{-1})	~1.3	~1.3	~1.3
Breakdown electric field at $N_D = 3 \times 10^{16}$ cm^{-3}				
$E_{B_{\parallel}}(c\text{-axis})$	(MV cm^{-1})	1.4	2.8	3.0
$E_{B_{\perp}}(c\text{-axis})$	(MV cm^{-1})	1.4	2.2	1.7
Relative dielectric constant				
$\varepsilon_{s_{\parallel}}(c\text{-axis})$	–	9.72	10.32	10.03
$\varepsilon_{s_{\perp}}(c\text{-axis})$	–	9.72	9.76	9.66
Thermal conductivity	(W cm^{-1} K^{-1})	3.3–4.9	3.3–4.9	3.3–4.9

typically consist of multiple layers to achieve excellent electrical performance, better high-temperature stability, good resistance to oxidation, etc. Taking the Pt/$TaSi_2$/Ti[19] metallization stack as an example, Ti is the Ohmic contact metal, Pt is the capping layer to enhance connectability to external circuitry (e.g., wire bonding), and $TaSi_2$ is a conductive diffusion barrier to prevent interdiffusion between Ti and Pt during high-temperature operation. Although Ohmic contacts to SiC have been widely investigated, low stable specific contact resistance, good resistance to oxidation, and the ability to be connected to external circuits are still highly desired characteristics.[25] This review focuses on recent progress in Ohmic contacts to SiC, including the current transport mechanism, the electrical properties, and especially the thermal stability of Ohmic contacts, as well as possible future research directions.

MECHANISM OF OHMIC CONTACT TO SIC

An Ohmic metal–semiconductor contact is defined as having a linear, symmetric current–voltage relationship for positive and negative voltages, and negligible resistance between metal and semiconductor as compared with the bulk resistance of a device. An Ohmic contact is typically formed in the following cases:

(I) The work function of a metal is matched to that of SiC; in other words, there is no potential barrier between the metal and SiC. For n-type SiC, the work function of the metal should be smaller than the electron affinity of SiC. Unfortunately, the work functions of almost all metals are in the range of 4.5 eV to 6 eV,[26] while the electron affinity of SiC is about 4 eV.[1,2] For p-type SiC, the valence band edge is more than 7 eV below the vacuum level.[27] However, no metal has a work function above 6 eV. As described above, it is hard to find an appropriate metal that can form an ideal contact to n- or p-type SiC.

(II) There is a quite low potential barrier between the metal and SiC. As a result, electrons can traverse the barrier at the interface. In this case, the specific mechanism of current flow is thermionic emission (TE), which can be described as follows[28,29] (taking n-type SiC as an example, similarly hereinafter):

$$J = J_0\left[\exp\left(\frac{qV}{nkT}\right) - 1\right] = A^*T^2\left[\exp\left(\frac{qV}{nkT}\right) - 1\right]\exp\left(\frac{-q\phi_B}{kT}\right), \quad (1)$$

$$J_R = A^{**}T^2\exp\left(-\frac{q\phi_B}{kT}\right)\left[1 - \exp\left(-\frac{qV_R}{kT}\right)\right], \quad (2)$$

where J/J_R is the forward/reverse current density per unit area, J_0 is the saturation current density, A^*/A^{**} is the effective Richardson constant for SiC/metal, T is absolute temperature, V/V_R is the applied forward/reverse bias, n is the ideality factor in the current–voltage I–V characteristic, and ϕ_B is the potential barrier height. The specific contact resistance is in general represented as

$$\rho_c = \left(\frac{\partial V}{\partial J}\right)_{V=0} = \left(\frac{k}{qA^*T}\right)\exp\left(\frac{q\phi_B}{kT}\right) \propto \exp\left(\frac{q\phi_B}{kT}\right). \tag{3}$$

Thus, the specific contact resistance increases exponentially as the potential barrier height ϕ_B increases. Han et al.[30] reported that the current transport mechanism of Ni to n-type 4H-SiC ($N_D = 4.2 \times 10^{15}$ cm^{-3}) could be described through the thermionic emission model. According to Eq. 3, when $\phi_B = 0.35$ V,[31] $A^* = 146$ A cm^{-2} K^{-2},[32] ρ_c was calculated to be 1.45×10^{-3} Ω cm^2, which was in good agreement with experimental data. To lower the specific contact resistance under these circumstances, Vassilevski et al.[33] reduced the height of the metal–SiC potential barrier to 0.097 eV, which enhanced the Ohmic contact performance greatly.

(III) There is a narrow potential barrier between the metal and SiC, which can be obtained by heavy doping of the near-contact region of silicon carbide. In this regard, electrons can penetrate the barrier by quantum-mechanical tunneling, and the specific mechanism of current flow is field emission (FE).[28,34] Then, the dependence of the forward current density J on the voltage V is exponential:

$$J = J_0 \exp\left(\frac{qV}{E_{00}}\right), \tag{4}$$

where E_{00} is the Padovani–Stratton parameter,[34] which is given by

$$E_{00} = \frac{qh}{4\pi}\sqrt{\frac{N_D}{m^*\varepsilon}}, \tag{5}$$

where q is the electronic charge, N_D is the donor concentration, h is the Planck constant, m^* is the effective electron mass, and ε is the dielectric permittivity of SiC.

$$J_0 = \frac{2\pi A^* E_{00}\exp\left(-\frac{q\phi_B}{E_{00}}\right)}{kT\left\{\log\left[2\left(\frac{V-\phi_B}{\xi}\right)\right]\right\}\sin\left\{\frac{\pi kT}{2E_{00}}\log\left[2\left(\frac{V-\phi_B}{\xi}\right)\right]\right\}}. \tag{6}$$

ξ is equal to $(E_F - E_V)/q$, E_F is the position of the Fermi level and E_V is the valence band edge.

When reverse bias is applied, the dependence of the reverse current density J_R on the voltage V_R is given by

$$J_R = \frac{\pi A^{**} E_{00}\exp\left[-\frac{2(q\phi_B)^{3/2}}{3E_{00}\sqrt{q\phi_B - qV_R}}\right]}{kT\sqrt{\frac{\phi_B}{\phi_B - V_R}}\sin\left[\frac{\pi kT\sqrt{\frac{\phi_B}{\phi_B - V_R}}}{E_{00}}\right]}. \tag{7}$$

The specific contact resistance can then be described as[35–37]

$$\rho_c = \left(\frac{\partial V}{\partial J}\right)_{V=0} = \left[\frac{\pi A^* qT^2}{k\sin(\pi ckT)}\exp\left(-\frac{q\phi_B}{E_{00}}\right) - \frac{A^* q}{ck^2}\exp\left(-\frac{q\phi_B}{E_{00}} + cq\xi\right)\right]^{-1}, \tag{8}$$

$$c = \frac{1}{2E_{00}}\ln\left(-\frac{4\phi_B}{\xi}\right). \tag{9}$$

Then,

$$\rho_c \propto \exp\left(\frac{\phi_B}{\sqrt{N_D}}\right). \tag{10}$$

In this way, the specific contact resistance exponentially increases with the decrease of the square root of the carrier concentration; For instance, Lundberg et al.[38] investigated two different donor concentrations in epilayers of n-type 6H-SiC, finding that the calculated ratio of specific contact resistance between ρ_c' ($N_D = 7 \times 10^{18}$ cm^{-3}) and ρ_c'' ($N_D = 1.4 \times 10^{19}$ cm^{-3}) through Eq. 10 was about 4, in line with the experimental values.

(IV) Combining the TE and FE mechanisms, electrons can also tunnel through the barrier as it thins towards the top in certain cases; the specific mechanism of current flow is thermal field emission (TFE),[34,39] which is depicted as follows:

$$J = J_0\exp\left(\frac{qV}{E_0}\right) = J_0\exp\left(\frac{qV}{E_{00}\coth\left(\frac{E_{00}}{kT}\right)}\right), \tag{11}$$

$$J_0 = \frac{A^*T\sqrt{\pi E_{00}q(\phi_B - V - \xi)}}{k\cosh\left(\frac{E_{00}}{kT}\right)}\exp\left(-\frac{q\xi}{kT} - \frac{q}{E_0}(\phi_B - \xi)\right), \tag{12}$$

$$J_R = J_{00}\exp\left(-\frac{qV_R\left(\frac{E_{00}}{kT} - \tanh\frac{E_{00}}{kT}\right)}{E_{00}}\right), \tag{13}$$

$$J_{00} = \frac{A^{**}\sqrt{\pi E_{00}}}{kT}\sqrt{-qV_R + \frac{q\phi_B}{\cosh^2\frac{E_{00}}{kT}}}\exp\left(-\frac{q\phi_B}{E_0}\right). \tag{14}$$

Hence, the specific contact resistance can be expressed as[36]

$$\rho_c = \frac{k\sqrt{E_{00}}}{qA^*T\sqrt{\pi q(\phi_B - \xi)}} \cosh\left(\frac{E_{00}}{kT}\right) \coth\left(\frac{E_{00}}{kT}\right) \times \exp\left(\frac{q}{E_0}(\phi_B - \xi) + \frac{q\xi}{kT}\right). \quad (15)$$

Then,

$$\rho_c = \left(\frac{\partial V}{\partial J}\right)_{V=0} \propto \exp\left(\frac{\phi_B}{\sqrt{N_D}\coth\left(\frac{E_{00}}{kT}\right)}\right). \quad (16)$$

Thus, the specific contact resistance increases exponentially with the increase of the potential barrier height ϕ_B and decrease of temperature. Using the TFE model, Nakamura et al.[40] successfully predicted the specific contact resistance from the barrier height (around 0.40 eV) for $NiSi_2$/*n*-type 6H-SiC, being well consistent with the measured values.

In fact, theoretical calculations[28] can predict the emission conditions for which a specific current flow mechanism plays the dominant role, showing that the main mechanisms are thermionic emission when $\frac{E_{00}}{kT} < 0.5$, thermal field emission when $0.5 < \frac{E_{00}}{kT} < 5$, and field emission when $\frac{E_{00}}{kT} > 5$.

SURFACE PREPARATION

According to the mechanism of Ohmic contact to SiC, the potential barrier height (ϕ_B) between the metal and SiC must be as low as possible to achieve good Ohmic contact, even if the depletion layer at the metal/SiC interface is thin enough that TFE or FE can take place. Schottky and Mott[41,42] theorized that the potential barrier height between a metal and SiC (taking *n*-type SiC as an example) is

$$q\phi_B = q\phi_m - \chi_s, \quad (17)$$

where $q\phi_B$ is the work function of the metal and χ_s is the electron affinity of SiC. Meanwhile, Bardeen et al.[43] considered that, if the density of surface states (D_s) is sufficiently high, the difference in work function between the metal and SiC is compensated by surface state charge (Fermi level pinning), thus the potential barrier height between the metal and SiC is

$$q\phi_B = E_g - q\phi_0, \quad (18)$$

where E_g is the bandgap of SiC and ϕ_0 is defined as the energy below which the surface states must be filled for charge neutrality at the SiC surface. Combing these Schottky–Mott and Bardeen theoretical models, Cowley et al.[44] derived the dependence of the potential barrier height on the metal work function and the density of surface states, being given approximately by

$$q\phi_B = \gamma(q\phi_m - \chi_s) + (1-\gamma)(E_g - q\phi_0), \quad (19)$$

where γ is a weighting factor which depends mainly on the density of surface states; when D_s is sufficiently high, γ is equal to 0, otherwise γ is equal to 1 as D_s is extremely low.

Based on the Cowley–Sze theoretical model, preparation of clean, atomically flat surfaces free of native oxides and other contaminants to reduce the density of surface states and thus lower the potential barrier height is a crucial step prior to SiC metallization. Various cleaning procedures including wet chemical cleaning (RCA, RCA-like, etc.), thermal oxidization followed by etching in dilute HF (O/E), plasma-based treatment, high-temperature annealing, etc. have been investigated to achieve an ideal SiC surface.[45–55] Unfortunately, wet chemical treatment or O/E often leaves a trace of O and/or F contamination[45–49] on the SiC surface, which causes the density of surface states to be too high ($> 10^{12}$ states cm^{-2} eV^{-1}), thus increasing $q\phi_B$, ascribed to partial Fermi level pinning at the metal/SiC interface.[47] Plasma-based methods such as Ar,[50] Cl_2,[51] and N_2 plasma treatment[55] can effectively remove oxygen from the SiC surface but can cause surface damage during high-temperature processing.[50] High-temperature hydrogen annealing is suitable for producing clean, atomically ordered, smooth surfaces through surface hydrogen termination without introducing contamination;[52–54] however, it requires precisely controlled high-temperature processing of SiC under ultrahigh-purity molecular hydrogen, which makes it infeasible for a low-cost production environment.[53,54] Teraji et al.[47] developed a novel, simple method to lower the density of surface states through immersion in boiling water after the conventional procedure of degreasing and HF dipping (DHF) and O/E treatment. The position of the interface Fermi level was close to the Schottky limit with density of surface states of 4.63×10^{10} states cm^{-2} eV^{-1}, lowering the potential barrier height for Ti/6H-SiC electrodes from 0.736 eV to 0.451 eV. Huang et al.[56,57] and Liu et al.[58] proposed a low-temperature (400°C) electron cyclotron resonance microwave hydrogen plasma treatment method for passivating 4H-SiC surfaces and releasing Fermi level pinning with extremely low density of surface states ($\sim 10^{10}$ states cm^{-2} eV^{-1}).

Due to the complicated formation mechanisms of Ohmic contact to SiC and difficulties in obtaining an ideal SiC surface with low density of surface states, the exact values of specific contact resistance are generally obtained from actual measurements by the transmission line model (TLM)[59] or circular transmission line model (c-TLM)[60] instead of theoretical calculations.

OHMIC CONTACTS TO *n*-TYPE SIC

Since Addamiano first studied Cr-based Ohmic contacts to *n*-type 6H-SiC in 1970,[61] intense studies

Table II. Ohmic contacts to *n*-type SiC

Metallization Stack	SiC Polytype	Doping Level ($\times 10^{18}$ cm^{-3})	Annealing Conditions			ρ_c ($\times 10^{-5}$ Ω cm^2)	Surface Preparation Conditions	Refs.
			Temperature (°C)	Time (min)	Atmosphere			
Ni	6H	0.0055	1070	10	Vacuum	>800	RCA-like	62
Ni/Ti	6H	0.45	960	10	Vacuum	500	Chem. clean./Ar^+ ions	63
C	4H	13	1050	30	Ar	431	Modified RCA	64
Ni	6H	1	1000	5	Ar	300	RCA	65
Ti/Sb/Ti	6H	0.35	960	10	Vacuum	~270	Chem. clean.	66
Ti	6H	0.35	960	10	Vacuum	~250	Chem. clean.	66
Ti	4H	1	No annealing			225	RCA/HPT	67
Ni/Ti	6H	0.47	1065	10	Vacuum	105	Chem. clean.	68
Pt/Si	6H	0.35	1065	15	Vacuum	100	Chem. clean.	69
Ni	6H	0.55	960	10	Vacuum	80	RCA-like	62
Si	6H	0.55	960	10	Vacuum	80	RCA-like	70
Ti/Sb/Ti	6H	2.3	960	10	Vacuum	~77	Chem. clean.	66
Ti/Al/Ti	6H	2.3	1065	10	Vacuum	73.6	Chem. clean./plasma clean.	71
Ni/Si	6H	15	300	540	N_2	69	RCA-like	72
Ti/TiN/Pt/Ti/Ti	4H	30	1050	N.R.	Ar	65	Piranha etched/HF	73
Ti	6H	2.3	960	10	Vacuum	~55	Chem. clean.	66
Ti_3SiC_2	4H	15	950	1	Ar	50	Chem. clean.	74
Si/WNi	4H	5–7	1100	60	Ar	50	Chem. clean.	75
C	4H	13	1350	30	Ar	43	Modified RCA	64
Ni	6H	1.7	960	10	Vacuum	42	Chem. clean./Ar^+ ions	63
TiW	4H	50	950	5	Ar	40.8	N.R.	76
Pt	4H	4.2	1150	15	Vacuum	40	Chem. clean.	69
Au/TaSiN/Ni/Si	4H	N.R.	1000	3	N_2	~40	Chem. clean.	77
Au/Ni/Si	4H	N.R.	1000	3	N_2	~40	Chem. clean.	77
Pt/$TaSi_x$/Ni	4H	11	950	30	Ar	35	Chem. clean./O/E	78
Pt/$TaSi_x$/Ni	4H	0.01	900	5	Ar	34	N.R.	21
Ni/Ti	6H	1.7	970	10	Vacuum	33	Chem. clean./Ar^+ ions	79
Ta/Ni/Ta	6H	0.6	800	10	Ar	30	Chem. clean.	80
WSi_2	6H	>10	1000	20	H_2	24	RCA/PECVD SiO_2/BOE	16
Ni/Ti	6H	19	960	10	Vacuum	22	Chem. clean./Ar^+ ions	63
Ti/TiN/Pt/Ti/Ni	4H	30	950	N.R.	Ar	21	Piranha etched/HF	73
Ti	4H	1	400	5	N_2	20.7	RCA/HPT	57
Co/C	4H	1.6	800	120	Vacuum	20.4	RCA/O/E	81
Al/Ti/Ni	4H	10	800	30	UHV	20	RCA/O/E	82
Al/Ni	4H	13	1000	5	UHV	18	HF	83
Ti/InN	4H	9.8	No annealing			18	RCA/O/E	84
Pt/$TaSi_2$/Ti	6H	7	600	30	N_2	16.8	Piranha etched/O/E	19
Nb	4H	3	1000	10	Vacuum	15.3	Chem. clean.	85
Ni	6H	19	960	10	Vacuum	15	Chem. clean./Ar^+ ions	63
Ni/C	4H	1.6	800	120	Vacuum	14.3	RCA/O/E	81

Table II. continued

Metallization Stack	SiC Polytype	Doping Level ($\times 10^{18}$ cm^{-3})	Annealing Conditions			ρ_c ($\times 10^{-5}$ Ω cm^2)	Surface Preparation Conditions	Refs.
			Temperature (°C)	Time (min)	Atmosphere			
SiN_x/SiO_y/Ti/Pt/TiN/Ti/Pt/$TaSi_x$/Ti/Ti	4H	20	1100	2	Ar	~12	Caro's acid/HF	86
SiN_x/SiO_y/Ti/Pt/TiN/Ti/Ti	4H	20	1100	2	Ar	~12	Caro's acid/HF	86
SiN_x/SiO_y/Ti/Pt/TiN/Ti/Ni	4H	20	1100	2	Ar	~12	Caro's acid/HF	86
SiN_x/SiO_y/Ti/Pt/TiN/Ti/Pt/$TaSi_x$/Ti/Ni	4H	20	1100	2	Ar	~11	Caro's acid/HF	86
Ni	4H	300	1000	1	N_2	~10	N.R.	87
Ta/Pt/Ta	N.R.	2	1000	5	Ar	9	Chem. clean.	88
Ni	4H	4.2	960	10	Vacuum	~8	Modified RCA	89
Ni/Si	4H	4.2	960	10	Vacuum	~8	Modified RCA	89
Si	4H	4.2	1070	10	Vacuum	7	RCA	70
Re	6H	1.28	1000	120	Vacuum	7.0	HF/acetone	90
Ta/Si	N.R.	N.R.	1050	30	N.R.	6	O/E	91
Ni/Ti	6H	2	950	2	Ar	5.9	RCA/HF	92
$MoSi_2$	6H	>10	1000	20	H_2	5.2	RCA/PECVD SiO_2/BOE	16
Pt/$TaSi_2$/Ni	6H	8.1	950	5	Vacuum	5.2	Chem. clean./HF	93
Pd	4H	4.2	1150	10	Vacuum	5.0	Chem. clean.	94
TiW/Ni	4H	5	975	1	N_2	4.2	RCA	95
Al/Ni/Ti	4H	10	1000	10	Ar	4.1	N.R.	96
Ni/Si/Ge	4H	4.2	960	10	Vacuum	4	RCA	97
Ta-Si	4H	6–8	950	3	Ar	4	Chem. clean.	98
Ni	6H	7.4	950	1	N_2	3.9	N.R.	99
TiW	4H	11	950	30	Vacuum	3.3	Chem. clean./ICP etched	100
W/WC/TaC	6H	8.1	1000	15	Vacuum	~3	Chem. clean.	17
TaC	6H	23	1000	15	Vacuum	2.1	Chem. clean./O/E	101
Cr/graphite	6H		No annealing			1.7	Alcohol/hydrogen etched	102
Pt/Ti/TiW	4H	11	950	30	Ar	1.5	Chem. clean./O/E	78
Pt/TaC	6H	7.8	1000	15	Vacuum	~1.4	Chem. clean./O/E	101
Ni/Si	4H	10	No annealing			1.3	RCA/SIP	103
Ni/C_{60}	4H	18	800	120	Ar	1.17	RCA/O/E	104
Pt/$TaSi_x$	4H	11	950	10	Ar	1	Chem. clean./O/E	78
Graphene	6H	10	No annealing			0.6	N.R.	105
Au/PtN/TaSiN/$Ni_{80}Cr_{20}$	4H	50	1000	2	Vacuum	~0.5	RCA	106
Ni	4H	1–3	950	5	Ar + 1% H_2	0.49	RCA/Ar^+ ions	107
Ni/Ti	4H	~100	950	1	N_2	0.48	RCA	108
Si/Al/Ti	4H	26	1020	2.5	Ar	0.37	O/E	109
Au/Ti/Al	4H	8–12	1050	5	Ar	0.28	RCA	110
Ni/Si	4H	2	900	10	Ar + 5% H_2	0.27	O/E	111

Table II. continued

Metallization Stack	SiC Polytype	Doping Level ($\times 10^{18}$ cm^{-3})	Annealing Conditions			ρ_c ($\times 10^{-5}$ Ω cm^2)	Surface Preparation Conditions	Refs.
			Temperature (°C)	Time (min)	Atmosphere			
Au/TaC	6H	7.8	1000	15	Vacuum	~0.2	Chem. clean./O/E	101
Co/Si/Co/Si/Co	4H	11	500 + 800	10 + 2	Ar + 10% H_2	0.18	Chem. clean.	112
Au/B_4C	N.R.	N.R.	1050	30	N.R.	0.15	O/E	91
Pt/TaC	6H	23	1000	15	Vacuum	~0.14	Chem. clean./O/E	101
Cu/Si/Cu	4H	11	500 + 850	10 + 1	Ar + 10% H_2	0.12	Chem. clean.	113
Ni/C	4H	31	800	120	Ar	0.0658	Chem. clean./O/E	114
Al-Si/TaN/Ta/Ni	4H	250	1000	2	Ar	0.04	N.R.	115

Multilayered contacts are designated with slashes to separate the distinct layers prior to annealing; layers are listed from right to left in deposition order (e.g., Pt/$TaSi_2$/Ti refers to Pt/$TaSi_2$/Ti/SiC).N.R. = not reported; UHV = ultrahigh vacuum; Chem. clean. = chemical cleaning; RCA = RCA cleaning; BOE = etching in HF-NH_4F solution; O/E = thermal oxidization followed by etching in diluted HF; HPT = hydrogen plasma treatment; SIP = silicon interlayer pretreatment. For annealing, "+" refers to a two-step annealing procedure (e.g., Temperature: 500 + 800 and Time: 10 + 2 refers to 500°C for 10 min followed by 800°C for 2 min).

over the past few decades have focused on Ohmic contacts to *n*-type SiC to obtain extremely low specific contact resistance and excellent oxidation-tolerant performance[16,17,19,21,57,62–115] (shown in Table II). To form Ohmic contacts, initially metals were usually heated to above their respective melting temperatures.[61] Obviously, such high annealing temperatures are unsuitable for practical applications. So far, an increasing number of researchers have turned to lower annealing temperatures. Jang et al.[101] investigated TaC contacts to *n*-type 6H-SiC; Ohmic contacts with $\rho_c = 2.1 \times 10^{-5}$ Ω cm^2 were obtained from substrates with $N_D = 2.3 \times 10^{19}$ cm^{-3} after rapid thermal annealing (RTA) in vacuum at 1000°C for 1 min. The specific contact resistance reached the lowest value (6.7×10^{-5} Ω cm^2) after annealing at 1000°C for Ti contacts to *n*-type 6H-SiC.[116] To date, the vast majority of studies have no choice but to anneal metal contacts to *n*-type SiC at reasonably high temperatures in the range from 800°C to 1100°C to obtain better Ohmic contact performance, thus it is hard to understand the Ohmic contact formation mechanism owing to the complicated interface reactions or metal interdiffusion. Different explanations for the low specific contact resistance have been proposed. Some researchers consider that the Ohmic behavior can be attributed to the formation of silicides and carbides such as $TiSi_2$ and Ni_2Si or diffusion of Si atoms into the metallization layers at elevated temperatures.[65,117–119] Also, some researchers consider that carbon vacancies are generated from outdiffusion of C atoms at the interface during the annealing process, acting as donors that play a key role in reduction of the effective Schottky barrier height and promote Ohmic contact formation.[120–122] However, others hold the different view that high-temperature annealing of Ni_2Si Ohmic contacts to *n*-type 4H-SiC appears to cause dissolution of the interfacial oxide and form an abrupt void-free metal/SiC interface, thereby attaining excellent electrical properties.[123,124] Hanafusa et al.[125] investigated the properties of Al/*n*-type 4H-SiC contacts with a crystallized amorphous-silicon interlayer, finding that the amorphous-silicon insertion layer was effective for Schottky barrier height reduction. Huang et al.[57] produced low-resistance Ti Ohmic contacts to *n*-type 4H-SiC through low-temperature electronic cyclotron resonance microwave hydrogen plasma pretreatment of the SiC surface, which released Fermi level pinning and thus decreased the surface state density, thereby lowering the specific contact resistance to 2.07×10^{-4} Ω cm^2 under low-temperature (400°C) annealing. Hertel et al.[105] verified the excellent electrical contact properties of graphene/*n*-type 6H-SiC interfaces, obtaining specific contact resistance of $\rho_c = 6 \times 10^{-6}$ Ω cm^2 ($N_D = 1 \times 10^{19}$ cm^{-3}) without annealing. They found that monolayer graphene contributed to the formation of Ohmic behavior in that work.

All in all, the mechanisms of Ohmic contact formation are rather complex, especially when metal/*n*-type SiC contacts are annealed at high temperature for a period. In general, according to the current transport mechanism of Ohmic contacts, once Ohmic contacts form between metal stacks and *n*-type SiC, decrease of the effective Schottky barrier height or increase of the charge carrier concentration in the near-contact region of *n*-type SiC, and thus narrowing of the Schottky barrier, should take place. There is still a long way to go to figure out the detailed mechanism of Ohmic contacts to *n*-type SiC.

OHMIC CONTACTS TO *p*-TYPE SIC

Shier et al.[126] first applied melting of Cu-Ti and Al-Si eutectic alloys to wet on *p*-type SiC (unknown polytype), forming Ohmic contacts. However, the contacts penetrated the SiC too deeply, and the specific contact resistance was too high. Recently, extensive studies have been carried out for Ohmic contacts to *p*-type SiC. The reported Ohmic contacts mainly include Al-based metal stacks, such as Al/Ti,[127–131] Ni/Ti/Al,[132–134] Ti-based alloys Ni/Ti,[108,135–137] Ni-based metal films such as Ni,[87,138] Al/Ti/Pt/Ni,[33] Au/Ta/TaRu/Ni,[139] metal carbides TiC,[140] or several kinds of noble-metal-based Ohmic contacts, for example, Au/Pd,[141] Pt,[142] Au/Pd/Ti/Pd,[143] etc. (summarized in Table III).[33,82,83,87,106,108,109,127–130,133,136,138–155] Tsukimoto et al.[133] investigated the electrical properties of Ni/Ti/Al contacts to *p*-type 4H-SiC after annealing in vacuum at 800°C for 30 min, which provided specific contact resistances of approximately 7×10^{-5} Ω cm^2. However, the vast majority of the aforementioned contacts were annealed at temperatures above 800°C to obtain relatively low specific contact resistance. Extreme annealing temperatures may cause stress in device structures[2] and also cause rough contact surface morphology,[156] which makes it difficult to align in the photolithography process. To reduce the annealing temperature, Lee et al.[140] developed epitaxial TiC Ohmic contacts to Al-ion-implanted 4H-SiC, achieving a relatively low specific contact resistance of 1.9×10^{-5} Ω cm^2 after annealing in Ar + 10% H_2 atmosphere for 3 min at 500°C. Tsukimoto et al.[157] added a small amount of Ge to the conventional binary Ti/Al contacts to construct ternary contacts, which yielded a specific contact resistance of approximately 1×10^{-4} Ω cm^2 after annealing at a temperature as low as 600°C for 30 min. Tsao et al. improved AlNi-based Ohmic contacts to *p*-type 4H-SiC by implanting low-energy Al^+ and inserting a thin Ti layer, which successfully decreased the specific contact resistance to 1.8×10^{-4} Ω cm^2 after annealing at 650°C for 30 min in Ar atmosphere.[158] Just like the Ohmic contact formation mechanism of *n*-type SiC, different explanations for Ohmic contact to *p*-type SiC have been proposed. One suggestion is that the Ohmic behavior is generated by formation of Ti_3SiC_2[159–161] or Al_3C_4.[129,162] The Schottky barrier height is reduced by the formation of the Ti_3SiC_2 layer, which acts as a *p*-type intermediate semiconductor layer at the metal/SiC interface.[157] Another suggestion is that Ohmic contacts (especially for Al-based contacts) exhibit pinning and/or spiking during high-temperature annealing,[127,163–165] which enhances the electric field by geometric effects, thus improving the performance of Ohmic contacts. Also, Crofton et al. assumed that aluminum diffuses into the SiC surface during annealing, resulting in a heavily doped layer at the interface, thus enhancing current transport by field emission.[25,166]

THERMAL STABILITY OF OHMIC CONTACTS

As discussed above, great efforts have been made to reduce the specific contact resistance of Ohmic contacts to SiC after annealing at certain temperatures. On the other hand, it is essential to achieve excellent thermal stability of Ohmic contacts to SiC in appropriate ambient conditions; otherwise continuous operation of SiC devices at high temperature would accelerate reactions between the contact materials and SiC substrate, or between individual contact layers, which would deteriorate the reliability of SiC devices.[122] As shown in Table IV, multilayered contacts, such as Au/CrB_2,[149] Pt/TaC,[101] W/WC/TaC,[17] Pt/Ir/Pt/$TaSi_2$/Ti,[167] Pt/Si,[146] TiW/Ni,[95] and Ni/Ti/Al/Ni[168] have been developed to maintain the thermal stability of Ohmic contacts to SiC. The specific contact resistance of CrB_2 Ohmic contacts to *p*-type 6H-SiC only increased slightly after 2226 h of aging at 300°C in vacuum.[149] Ohmic contacts comprising a W/WC/TaC/SiC multilayer sequence showed excellent thermal stability after storage testing at 600°C for 1000 h, with no degradation of specific contact resistance and no reaction among the films and *n*-type 6H-SiC substrate being observed.[17] However, long-term survivability of Ohmic contacts in vacuum or inert ambient is invalid in air atmosphere. Oxygen in air would lead to severe electrical and morphological degradation of Ohmic contacts due to severe oxidation; For example, Au/TiW/Ni_2Si contacts to *n*-type 6H-SiC showed little change in electrical characteristics up to 600°C in vacuum, while this metallization showed electrical degradation due to severe oxidation at 600°C when exposed to oxygen.[169] In this regard, a conductive diffusion barrier that can prevent diffusion of oxygen into the contacts during high-temperature aging as well as interdiffusion between Ohmic contact metals such as Ni or Ti and capping layers such as Pt or Au is essential for long-term reliability of SiC devices. Various diffusion barriers, for instance, $TaSi_x$,[19,21,78,93,167] WSi,[170] $TaRuN_x$,[139,150] TaSiN,[77,106] TaN,[115] and TiN,[73,86] are intended to slow the diffusion and/or reaction between adjacent layers greatly. Metallization stacks Au/Ta/TaRu/Ni/Al to *p*-type 4H-SiC substrates remained stable

Table III. Ohmic contacts to *p*-type SiC

Metallization Stack	SiC Polytype	Doping Level ($\times 10^{18}$ cm^{-3})	Annealing Conditions: Temperature (°C)	Annealing Conditions: Time (min)	Annealing Conditions: Atmosphere	ρ_c ($\times 10^{-5}$ Ω cm^2)	Surface Preparation Conditions	Refs.
Ni/Al	4H	7.2	1000	5	UHV	1200	HF	83
Ni/Ti/Al	4H	4.5	800	30	UHV	220	RCA/O/E	82
Ni/Ti	4H	~100	950	~1	N_2	130	RCA	108
Ni	4H	100	1000	1	N_2	~100	N.R.	87
Au/NiAl/ Ti/Ge	4H	>100	600	30	Vacuum	~80	N.R.	144
Au/NiAl/Ti	4H	>100	600	30	Vacuum	~50	N.R.	144
Al	4H	4.8	1000	2	Vacuum	42	N.R	129
Ti/Al	6H	16	900	4	N_2	40	N.R.	128
Co/Si/Ti	4H	3.9	850	1	Vacuum	40	Chem. clean.	145
Pt/Si	6H	7	1100	5	Vacuum	28.9	Chem. clean.	146
Al/Ti/Al	4H	4.8	1000	2	Vacuum	25	N.R.	129
Au/Pt-N/ TaSiN/ $Al_{70}Ti_{30}$	4H	~1000	1000	2	Vacuum	~20	RCA	106
Si/Al/Ti	4H	24	1020	2.5	Ar	17	BHF	109
Pt	4H	10	1100	5	Vacuum	~15	Chem. clean.	142
Al/Ti/Ge	4H	4.5	600	30	Vacuum	10.3	RCA/O/E	147
AlSiTi	4H	30–50	950	7	Ar	9.6	RCA/Ar^+ ions	148
Au/CrB_2	6H	13	1100	15	Vacuum	9.58	Chem. clean.	149
Ni/Pt/Ti/Al	4H	6–8	1000	2	Vacuum	9	RCA	33
Al/Ti/Ni	4H	4.5	800	30	Vacuum	7	Chem. clean./O/E	133
Au/Pt-N/ TaSiN/ Ni (7% V)	4H	~1000	900	1	Vacuum	~8	RCA	106
Ti/Al	4H	10	1000	2	Vacuum	~7	Chem. clean.	142
Al/W	4H	100	850	1	Ar	6.8	RCA	130
Au/Sn/Pt/ TaRuN/Ni/Al	4H	1000	N.R.	N.R.	N.R.	2	Chem. clean.	150
W/NiAl/Ti	4H	>100	975	2	Ar	~5.5	N.R.	144
Pd	4H	50	700	N_2	5	5.5	Chem. clean./Ar^+ ions	151
Al/Ti	4H	100	850	1	Ar	4.8	RCA	130
Pt/Si	4H	10	1000	5	Vacuum	~4.4	Chem. clean.	142
Au/Pd	4H	30–50	850	15	Ar	4.19	RCA/Ar^+ ions	141
Au/Pd/Al	4H	30–50	900	5	Ar	4.08	RCA/Ar^+ ions	141
W/Ni/Al	N.R.	10	850	2	N.R.	4	Chem. clean.	152
Ni	4H	100	1000	1	Ar	~3	RCA	138
Au/Pd/Ti/Pd	4H	30–50	900	N.R.	Ar + 1% H_2	2.9	N.R.	143
Au/Ta/ TaRu/Ni	4H	~1000	850	1	Ar	~2	Chem. clean.	139
TiC	4H	20	500	3	Ar + 10% H_2	2	Chem. clean.	140
Ti/Al	4H	4.5	1000	2	Vacuum	2	Chem. clean./O/E	133
Au/TiW/Ti/Pd	4H	100	400 + 850	1.5 + 1	N_2	1.6	BOE	153
Au/Ti/Al	4H	30–50	900	5	Ar + 1% H_2	1.42	RCA/Ar^+ ions	154
Al-Ti	N.R.	13	1000	2	Vacuum	1.1	Chem. clean.	127
Au/Ru/ TaRu/Ni/Al	4H	~1000	850	1	Ar	~1	Chem. clean.	139
Al/Ti/Al	4H	10	1050	10	N.R.	0.5	RCA/Piranha etched/BOE	136
Al/Ti	4H	10	1050	N.R.	Ar	0.1	RCA-like	155

Multilayered contacts are designated with slashes to separate the distinct layers prior to annealing; layers are listed from right to left in deposition order. BHF = buffered hydrofluoric acid.

when aged at 350°C in air for 3000 h, with the specific contact resistance changing slightly from 1×10^{-5} Ω cm^2 to 2×10^{-5} Ω cm^2.[139] Okojie et al.[19] reported that Ti-based metallization films (Pt/$TaSi_2$/Ti to *n*-type 4H- and 6H-SiC) could successfully withstand 1000 h at 600°C in air. Oxidation

Table IV. Summary of results pertaining to thermal stability of Ohmic contacts to SiC in various atmospheres

Metallization Stack	Stack Thicknesses (nm)	Aging Conditions			Beginning of Test ($\times 10^{-5}$ Ω cm^2)	End of Test ($\times 10^{-5}$ Ω cm^2)	Refs.
		Temperature (°C)	Time (h)	Atmosphere			
Pt/$TaSi_2$/Ni	150/50/100	300	1000	Air	34.4	280	21
Au/CrB_2	200	300	2226	Vacuum	9.58	19.2	149
Al-Si/TaN/Ta/Ni	850/150/50/50	300	12,000	Ar	0.04	~0.04	115
Au/Sn/Pt/TaRuN/Ni/Al	200/25/100/200/50/15	350	2000	Air	2	3	150
Au/Ta/TaRu/Ni	700/5/200/50	350	3000	Air	~2	~4	139
Au/Ta/TaRu/Ni/Al	700/5/200/50/15	350	3000	Air	~1	~2	139
Au/Pt-N/TaSiN/$Al_{70}Ti_{30}$	N.R.	350	4000	Air	~20	~24	106
Au/Pt-N/TaSiN/Ni (7% V)	N.R.	350	4000	Air	~8	~8	106
Au/Pt-N/TaSiN/$Ni_{80}Cr_{20}$	N.R.	350	4000	Air	~0.5	~2.5	106
Al-Si/TaN/Ta/Ni	850/150/50/50	385	12,000	Ar	0.04	~0.06	115
Al/Ti/Ge	144/32/24	400	10	Ar	~10	~12	147
Au/Ni/Si	150/66/60	400	50	Air	~40	~80	77
Au/TaSiN/Ni/Si	150/100/66/60	400	50	Air	~40	~44.8	77
Ni	100	400	95	N_2	~10	~10	87
TiW/Ni	200/100	400	100	N_2	4.2	76	95
Pt/TaC	10/320	400	144	Vacuum	~1.4	~1.6	101
Au/TaC	10/320	400	144	Vacuum	~0.20	~0.24	101
$MoSi_2$	500	400	1000	Air	5.2	1.7	16
WSi_2	500	400	1000	Air	24	11	16
Al-Si/TaN/Ta/Ni	850/150/50/50	438	7000	Ar	0.04	~0.3	115
Au/Ti/Al	100/150/150	500	20	Ar	Stable		110
Pt/$TaSi_x$	400/200	500	45	20% O_2 in N_2	1.0	1.6	78
Pt/$TaSi_x$/Ni	400/200/100	500	70	20% O_2 in N_2	35	37	78
Pd	100	500	100	N_2	5.7	5.7	151
Ti/Al	60/40	500	100	N_2	1.42	2.1	107
Pt/Ti/TiW	300/30/180	500	520	20% O_2 in N_2	1.5	50	78
Pt/Ir/Pt/$TaSi_2$/Ti	200/200/200/400/100	500	1000	Air	N.R.	N.R.	167
SiN_x/SiO_y/Ti/Pt/TiN/Ti/Pt/$TaSi_x$/Ti/Ti	250/250/20/150/10/20/70/200/50/30	500	1000 + 1000	Air + air/10% moisture	~12	~53	86
SiN_x/SiO_y/Ti/Pt/TiN/Ti/Pt/$TaSi_x$/Ti/Ni	250/250/20/150/10/20/70/200/20/50	500	1000 + 1000	Air + air/10% moisture	~11	$>10^7$	86
SiN_x/SiO_y/Ti/Pt/TiN/Ti/Ti	250/250/20/150/10/20/30	500	1000 + 1000	Air + air/10% moisture	~12	~25	86
SiN_x/SiO_y/Ti/Pt/TiN/Ti/Ni	250/250/20/150/10/20/50	500	1000 + 1000	Air + air/10% moisture	~12	~30	86
Pt/$TaSi_2$/Ni	150/50/100	600	24	Air	87	2300	93
Pt/Si	60/50	600	60	Vacuum	Stable		146

Table IV. continued

Metallization Stack	Stack Thicknesses (nm)	Aging Conditions			Beginning of Test ($\times 10^{-5}$ Ω cm^2)	End of Test ($\times 10^{-5}$ Ω cm^2)	Refs.
		Temperature (°C)	Time (h)	Atmosphere			
AlSiTi	100	600	100	N_2	9.6	9.6	148
Ni	150	600	100	N_2	~0.5	~0.5	107
W/Ni/Al	200/200/200	600	300	Vacuum	Stable		152
Ni/Si	N.R.	600	300	Air	69	3.5	72
Pt/$TaSi_2$/Ni	200/400/100	600	300	Air	5.2	33	93
a-SiC/a-SiO_x/ Ti/Pt/TiN/Ti/ Ti	250/250/ 20/150/10/20/ 30	600	500	Air	~6.5	~22.9	73
a-SiC/a-SiO_x/ Ti/Pt/TiN/Ti/ Ti	250/250/ 20/150/10/20/ 30	600	500	Air/10% moisture	~6.5	~12.5	73
Ti/TiN/Pt/Ti/Ni	20/10/150/20/50	600	500	Air	~21	~17,900	73
Ti/TiN/Pt/Ti/Ti	20/10/150/20/30	600	500	Air	~65	~229	73
Ti/TiN/Pt/Ti/Ti	20/10/150/20/30	600	500	Air/10% moisture	~65	~125	73
W/WC/TaC	50/10/100	600	1000	Vacuum	Stable		17
Pt/$TaSi_2$/Ti	200/400/100	600	1000	Air	16.8	N.R.	19
Au/Ti-Al	100/200	700	100	N_2	Stable		154
Ni/Ti	50/10	900	10	H_2	33	~26	79
Si/WNi	20/100	1000	15	Ar	N.R.	50	75
W/WC/TaC	50/10/100	1000	1000	Vacuum	3.02	75.1	17

Multilayered contacts are designated with slashes to separate the distinct layers prior to annealing; layers are listed from right to left in deposition order (e.g., Ti/TiN/Pt/Ti/Ni refers to Ti/TiN/Pt/Ti/Ni/SiC).“+” refers to sequential aging procedures (e.g., Aging time: 1000 + 1000 and Aging atmosphere: Air + air/10% moisture refers to aging in air for 1000 h followed by 1000 h in air/10% moisture).

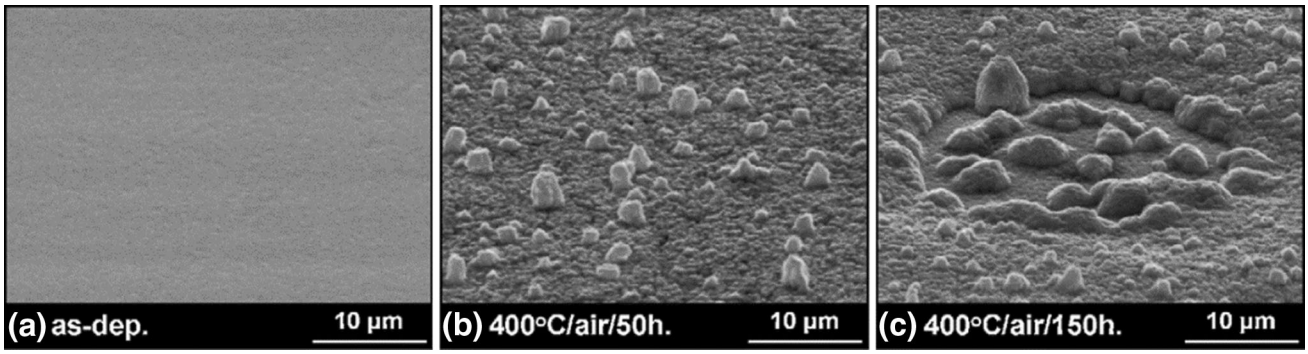

Fig. 1. SEM micrographs of Au/Ni_2Si/*n*-SiC Ohmic contacts: (a) as deposited, and aged in air at 400°C for (b) 50 h and (c) 150 h (after Ref. 20).

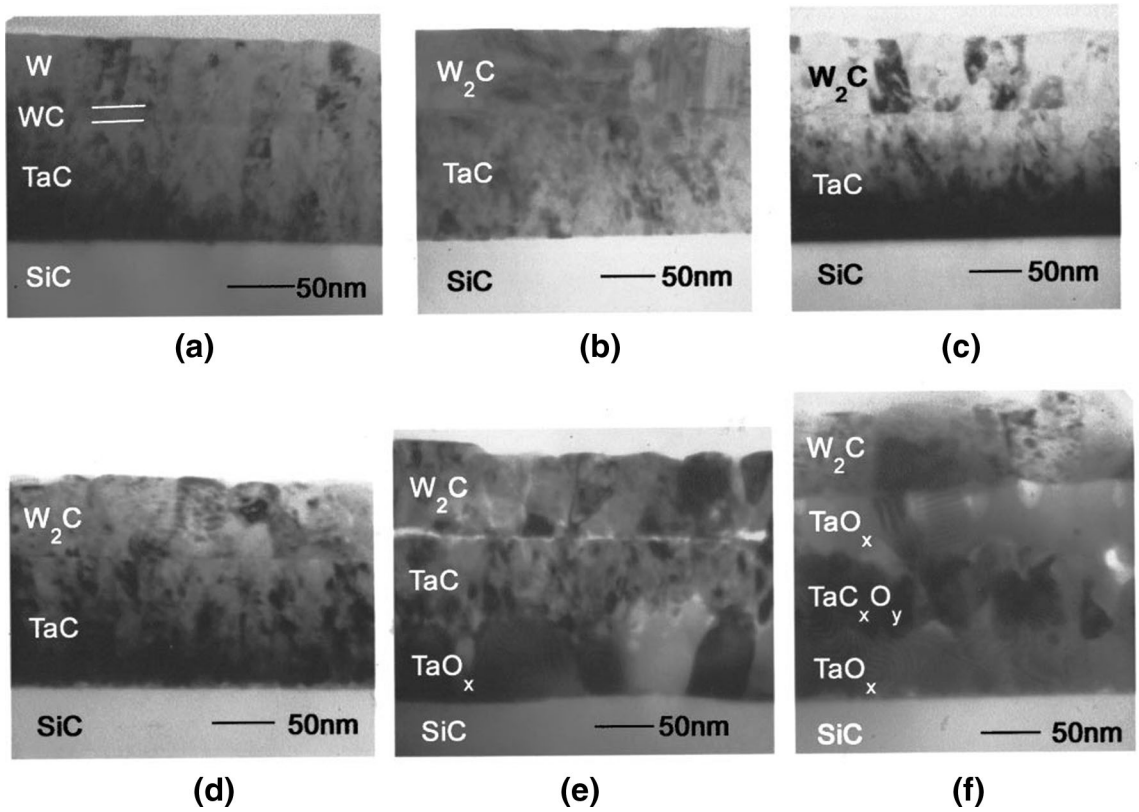

Fig. 2. Cross-sectional transmission electron microscopy (TEM) image of W/WC/TaC/SiC: (a) as deposited, and annealed at 1000°C for (b) 600 h, (c) 700 h, (d) 800 h, (e) 900 h, and (f) 1000 h (after Ref. 17).

resistance of Ohmic contacts still remains challenging when considering harsh moist operation environments; For example, oxidation is aggravated in combustion and exhaust gas environments.[171] Recently, many thermal stability tests performed in moist circumstances have been reported. Daves et al.[86] developed a novel approach to achieve the required stability, consisting of depositing stable protective coatings on the contact metallization, thus preventing penetration of oxygen into the contact region. In that work, SiN_x/SiO_y protective coatings were utilized on Ti-based Ohmic contacts to construct a SiN_x/SiO_y/Ti/Pt/TiN/Ti lamellar structure, and this system successfully withstood 1000 h of thermal treatment at 500°C in air and 1000 h of storage at 500°C in air/10% moisture. In another article,[73] a PECVD a-SiO_x/a-SiC protective coating successfully inhibited diffusion of oxygen/moisture into Ti-based contact metallization, with excellent stability being obtained during 500 h, long-term aging in both air and air/moisture at 600°C.

THERMAL DEGRADATION MECHANISM OF OHMIC CONTACTS DURING LONG-TERM AGING

Marinova et al.[172] studied the interface properties of Ni/*n*-type 6H-SiC and found that the formation of

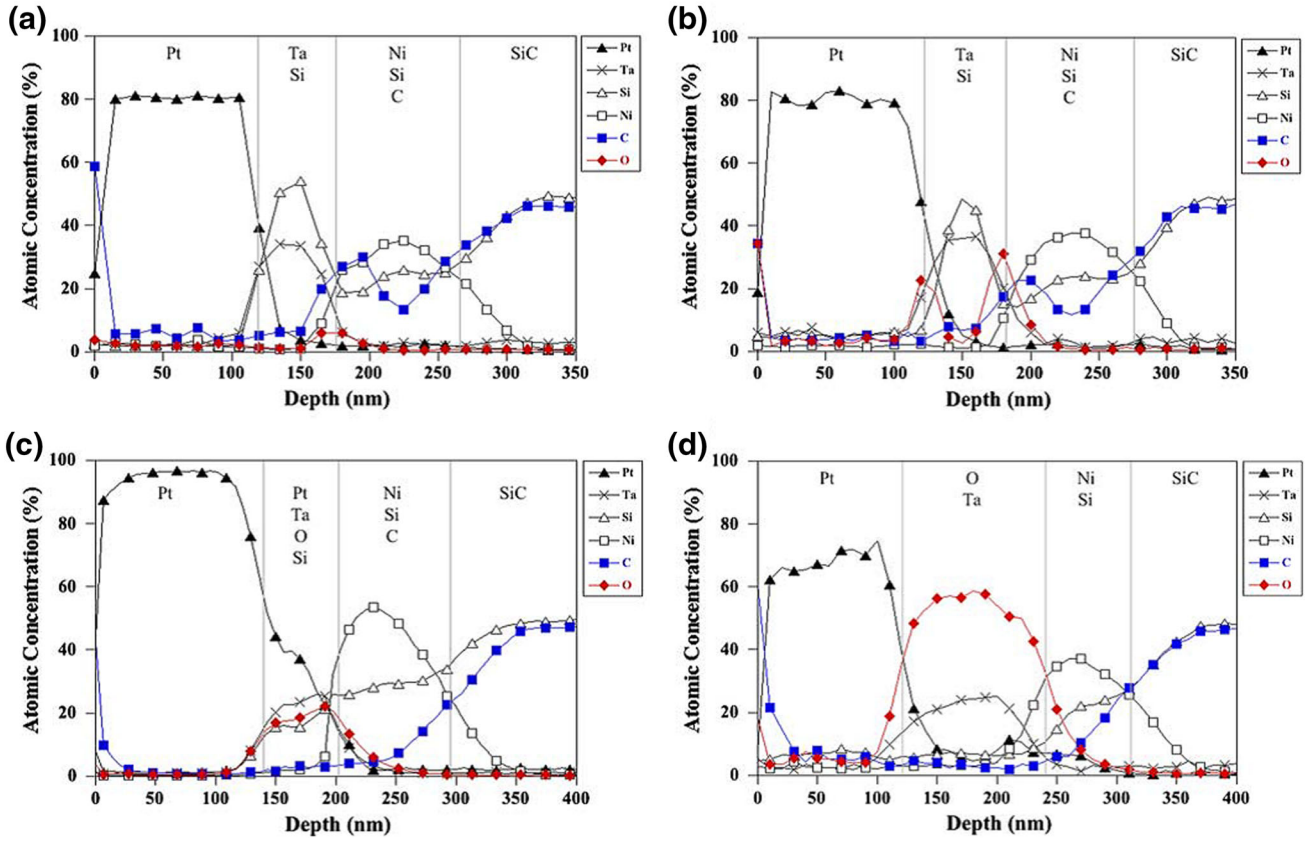

Fig. 3. AES depth profiles of (a) as-received Pt/TaSi$_x$/Ni Ohmic contacts with thickness of 150 nm/50 nm/100 nm, and contacts heated in air (b) at 300°C for 288 h, (c) at 500°C for 240 h, and (d) at 600°C for 48 h (after Ref. 21).

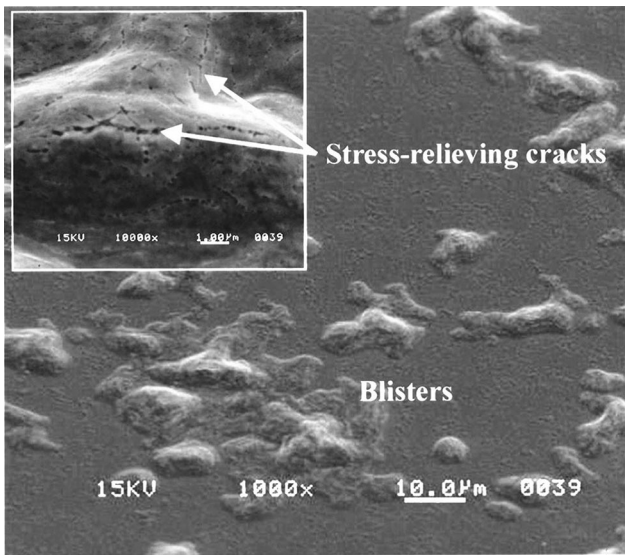

Fig. 4. SEM micrograph of Pt/TaSi$_2$/Ti Ohmic contacts with thickness of 300 nm/200 nm/100 nm after heat treatment in air at 600°C for 250 h (after Ref. 19).

unwanted Kirkendall voids at the interface after high-temperature annealing would undoubtedly cause internal stress and delamination of the contact layers, thereby resulting in thermal degradation. Kuchuk et al.[20,77] reported that Au/Ni$_2$Si Ohmic contacts aged in air at 400°C for 50 h tripled their specific contact resistance, and even presented non-Ohmic behavior after 150 h of aging. For 150-h-aged contacts, a mass of Au atoms diffused into the contact, while Ni and Si atoms diffused outward to the surface, leading to decomposition of the Ni$_2$Si phase and formation of NiSi and Au$_x$(Ni,Si)$_{1-x}$ phases. Then, oxygen penetrated into the contact through granular areas and craters appearing in the Au layer according to Fig. 1, resulting in corresponding electrical degradation. Baeri et al.[173] characterized the thermal stability of TiW films as diffusion barriers between a gold overlayer and the Ni$_2$Si/SiC Ohmic contact and found that Ti atoms diffused through the gold layer and reacted with oxygen to form a thin TiO$_x$ layer on aging in vacuum, damaging the performance of the Ohmic contact as well as the bondability in subsequent wire bonding. In most cases, electrical degradation during long-term aging of Ohmic contacts is due to oxidation.[17,19,21,93,101] Jang et al.[17] investigated the thermal stability and degradation mechanisms of TaC Ohmic contacts with W/WC overlayers to n-type 6H-SiC after annealing at 1000°C for 600 h, 700 h, 800 h, 900 h, and 1000 h in vacuum below 3×10^{-7} Torr. With increasing aging time, the W$_2$C/TaC and TaC/SiC interfaces became slightly roughened (Fig. 2d), then

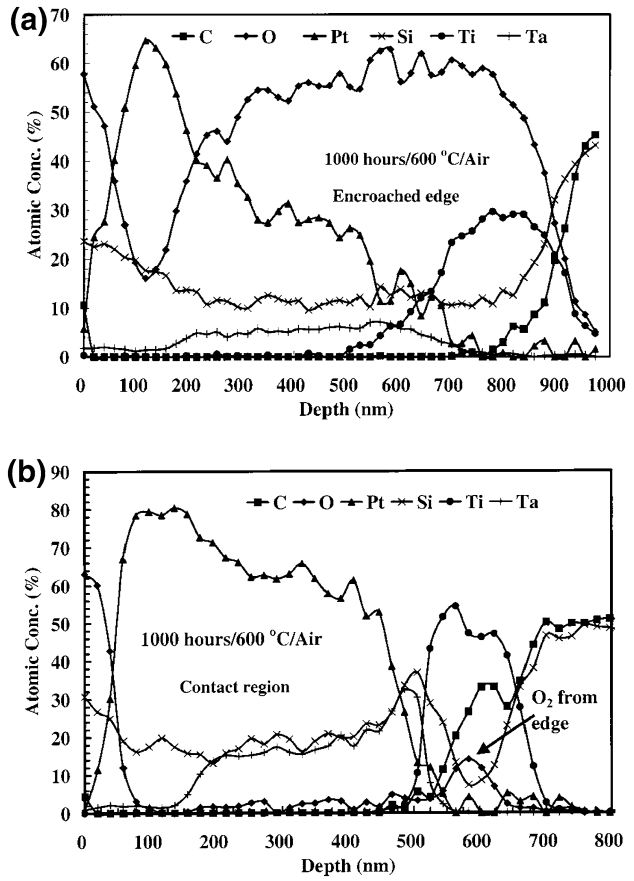

Fig. 5. AES depth profile of Pt (200 nm)/$TaSi_2$ (400 nm)/Ti (100 nm) Ohmic contact on SiC after 1000 h of heat treatment at 600°C in air (after Ref. 19).

generated new insulating phases (Fig. 2e). Finally, the TaC film decomposed completely to form oxide layers (Fig. 2f). Correspondingly, a substantial increase of the specific contact resistance to $8.08 \times 10^{-5}\ \Omega\ cm^2$ and $7.51 \times 10^{-4}\ \Omega\ cm^2$ occurred after 900 h and 1000 h of annealing, respectively. These results showed that the oxide phases nucleated first at the interfaces of contact layers, then grew together. Similarly, Pt/$TaSi_x$/Ni Ohmic contacts with thickness of 150 nm/50 nm/100 nm showed a large increase in specific contact resistance after aging at 300°C for 288 h in air, and non-Ohmic behavior after aging at 500°C for 240 h or 600°C for 36 h. The concentration profiles from Auger electron spectroscopy (AES) illustrated in Fig. 3 show that oxygen accumulation at interfaces could be responsible for the degradation, with the entirely oxidized tantalum silicide layer leading to electrical failure.[21] What is worse, thinner diffusion barriers could accelerate free Ohmic contact metals such as Ti to migrate to the surface and agglomerate locally at the diffusion barriers' (e.g., $PtSi_2$) subsurface, further causing formation of blisters and cracks (as seen in Fig. 4), which possibly provides a rapid diffusion path for oxygen towards the contact region.[19] To further improve the thermal stability, thicker Pt/$TaSi_x$/Ni contacts, with thickness of 200 nm/400 nm/100 nm, were employed in Ni-based Ohmic contacts to *n*-type 6H-SiC for high-temperature applications, showing only a gradual increase from an initial value of $5.2 \times 10^{-5}\ \Omega\ cm^2$ to $3.3 \times 10^{-4}\ \Omega\ cm^2$ after aging at 600°C for 312 h in air atmosphere. Use of a thicker $TaSi_2$ diffusion barrier and Pt capping layer substantially slowed the kinetics of oxygen diffusion/reaction within contact layers.[93] However, thicker Ohmic contacts could not effectively prevent extensive oxidation through the encroaching edge, even though no oxygen penetrated from the top layer (Fig. 5). Subsequent encroachment of oxygen into the active circular contact regions would cause electrical failure of the contact, especially during high-temperature (>500°C) annealing.[19]

CONCLUSIONS AND FUTURE PERSPECTIVES

This paper summarizes the development of Ohmic contacts to SiC and also emphasizes improvements and breakthroughs in the thermal stability of Ohmic contacts to SiC in recent years. To provide good Ohmic contacts to SiC, decreasing the effective Schottky barrier height or increasing the carrier concentration of SiC substrates is indispensable to lower the specific contact resistance. In addition, to improve the thermal stability of Ohmic contacts to SiC, better design of metal stacks on SiC and stable protective coatings are even more urgent.

In the past few decades, although significant progress has been made in the area of Ohmic contacts to SiC, there are still many challenges that have to be solved before SiC electronic devices can be put into practical high-temperature applications. To promote the commercialization process of high-temperature SiC devices, future work should focus on the following points:

1. Secondary Ohmic contacts: Secondary Ohmic contacts result when annealing of primary Ohmic contacts (such as Ni, Si) results in a structure that has very good electrical performance itself; these are then etched off, followed by deposition of a second metal with other required properties, such as excellent thermal stability, better oxidation resistance, good adhesion to SiC, etc. Moreover, the electrical performance of unannealed secondary contacts is nearly identical to that of the previous annealed ones.[94,174] Secondary Ohmic contacts can be optimized to improve the reliability of SiC devices for various applications, especially in aggressive environments. Some researchers are developing this kind of Ohmic contact.[70,94,174–177] Cichon et al. reported that $NiSi_2$ and Si secondary contacts showed good electrical properties and high thermal stability in air at 300°C for hundreds of hours.[177]
2. Bondable metallization stacks: Although some thermally stable Ohmic contacts such as

$Pt/TaSi_2/Ti$ can successfully withstand 1000 h of thermal treatment at 600°C in air,[19] detrimental silicides will inevitably form on the surface of Ohmic contacts after high-temperature aging, making the wire-bonding process for electronic packaging difficult. In this regard, it is necessary to develop bondable metallization stacks which can improve the success rate of wire bonding. Spry et al.[167] investigated Pt/Ir/$Pt/TaSi_2$ layers as both a bond metal and diffusion barrier, where the iridium layer prevents outdiffusion of silicon due to its inertness against formation of silicides during further aging, thus leaving a pure platinum layer at the surface, being ideal for the gold wire-bonding process.

3. Reproducible specific contact resistance results: The specific contact resistance usually varies under similar annealing conditions and similar carrier concentrations for Ni-based Ohmic contacts to *n*-type SiC.[65,94,99,107] In fact, the obtained specific contact resistance is determined by many factors, for example, the surface state density of SiC,[57] or even the model used to extract specific contact resistance data.[73] Therefore, an empirical formula including various influencing factors is urgently needed to calculate the specific contact resistance and further guide efficient research on Ohmic contacts.
4. Better electrical properties after mild annealing conditions: Most Ohmic contacts to SiC are annealed at temperatures above 800°C to achieve low specific contact resistance and relatively good thermal stability. Extreme annealing temperatures may cause a variety of issues. To date, one must make a trade-off between lower annealing temperature (<800°C) and better electrical performance in most cases. Some researchers have obtained moderate specific contact resistance values after low-temperature or even no annealing.[19,57,84,103,105] However, such low specific contact resistance values are generally obtained through decreasing the surface state density, which will restrict various industrial applications. In this regard, great efforts should be made to achieve better electrical properties using mild annealing conditions.
5. Simultaneous formation of *n*- and *p*-type Ohmic contacts: For SiC MOSFET devices, simultaneous formation of Ohmic contacts on both n^+-source and *p*-well regions using a single metal (or metal stack) in a one-step annealing process is really needed and will not only simplify device fabrication processes but also miniaturize cell sizes.[82,83,108,178] Although many materials have been investigated to form Ohmic contacts to *n*- or *p*-type SiC separately, only a few materials such as Ni,[179] Al/Ni,[83,178] Al/Ti/Ni,[82] Ni/Ti,[108] and W-Ni alloy[180] have been developed to form Ohmic contacts to both *n*- and *p*-type SiC. Due to the large difference in Schottky barrier height of metal/*n*-type and metal/*p*-type SiC for the same contact material, it is hard to obtain excellent Ohmic contact performance simultaneously. Moreover, the mechanisms of simultaneous formation of *n*- and *p*-type Ohmic contacts are not very clear, even though some researchers consider that δ-$Ni_2Si(Al)$[83] or W_xC_y-Ni_xSi_y[180] is responsible for simultaneous Ohmic contact formation.
6. Better optimization of Ohmic contact processing: According to the mechanism of Ohmic contacts to SiC, increasing the carrier concentration of the SiC substrate is an excellent strategy to achieve better Ohmic contact performance. In this case, ion implantation becomes a critical technique for selective-area doping during Ohmic contact processing due to the extremely low diffusion coefficients of dopants in SiC.[181] At the same time, ion implantation inevitably introduces a high density of defects and lattice disorder in the implanted region.[182,183] Thus, hot implantation and postimplantation high-temperature annealing are necessary to repair such implantation-induced damage and also to obtain high dopant activation.[184–186] However, these high-temperature annealing processes will cause surface roughening,[187–190] macrostep formation,[189] and/or dopant redistribution.[191,192] Several techniques to suppress the surface deterioration have been developed, such as annealing in silane,[190] annealing with an AlN[193] and/or graphite cap,[194] and rapid thermal annealing such as flash-lamp annealing[184] or laser-pulse-exposure-generated shock-wave annealing.[195] Despite the high-temperature processes, high sheet resistance of implanted layers is another major obstacle to Ohmic contact process technology, especially for *p*-type layers, which is due to incomplete dopant activation or low hole mobility.[196,197] Hence, to go one step further, great efforts should be made to optimize implantation and annealing techniques to obtain sufficient electrical activation with high surface quality and low sheet resistance.

ACKNOWLEDGEMENTS

This research was supported by the National Natural Science Foundation of China under Grant 51374084 and by grants from the Power Electronics Science and Education Development Program of Delta Environmental & Educational Foundation.

REFERENCES

1. T. Kimoto and J.A. Cooper, *Fundamentals of Silicon Carbide Technology* (Singapore: Wiley, 2014), pp. 11–33.
2. L.M. Porter and R.F. Davis, *Mater. Sci. Eng. B* 34, 83 (1995).
3. P.L. Dreike, D.M. Fleetwood, D.B. King, D.C. Sprauer, and T.E. Zipperian, *IEEE Trans. Compon. Packag. B* 17, 594 (1994).

4. J. Casady and R.W. Johnson, *Solid-State Electron.* 39, 1409 (1996).
5. V. Chelnokov, *Mater. Sci. Eng. B* 11, 103 (1992).
6. M. Ruff, H. Mitlehner, and R. Helbig, *IEEE Trans. Electron Devices* 41, 1040 (1994).
7. Y.B. Luo, J.H. Zhang, P. Alexandrov, L. Fursin, J.H. Zhao, and T. Burke, *IEEE Electron Device Lett.* 24, 695 (2003).
8. J.H. Zhao, P. Alexandrov, J. Zhang, and X. Li, *IEEE Electron Device Lett.* 25, 474 (2004).
9. P.G. Neudeck, D.J. Spry, L.Y. Chen, C.W. Chang, G.M. Beheim, R.S. Okojie, L.J. Evans, R.D. Meredith, T.L. Ferrier, and M.J. Krasowski, *Mater. Sci. Forum* 615, 929 (2009).
10. C.E. Weitzel, J.W. Palmour, C.H. Carter Jr, and K.J. Nordquist, *IEEE Electron Device Lett.* 15, 406 (1994).
11. S. Sriram, R. Clarke, A. Burk, H. Hobgood, P. McMullin, P. Orphanos, R. Siergiej, T. Smith, C. Brandt, and M. Driver, *IEEE Electron Device Lett.* 15, 458 (1994).
12. J. Palmour, H. Kong, and R. Davis, *Appl. Phys. Lett.* 51, 2028 (1987).
13. S.T. Sheppard, M.R. Melloch, and J.A. Cooper Jr., *IEEE Trans. Electron Devices* 41, 1257 (1994).
14. Y. Sui, X. Wang, and J.A. Cooper, *IEEE Electron Device Lett.* 28, 728 (2007).
15. Q. Zhang, M. Das, J. Sumakeris, R. Callanan, and A. Agarwal, *IEEE Electron Device Lett.* 29, 1027 (2008).
16. K. Gottfried, J. Kriz, J. Leibelt, C. Kaufmann, and T. Gessner, *High-Temperature Electronic Materials, Devices and Sensors Conference*, vol. 153 (1998).
17. T. Jang, B. Odekirk, L.D. Madsen, and L.M. Porter, *J. Appl. Phys.* 90, 4555 (2001).
18. M.W. Cole, P.C. Joshi, C. Hubbard, J.D. Demaree, and M. Ervin, *J. Appl. Phys.* 91, 3864 (2002).
19. R.S. Okojie, D. Lukco, Y.L. Chen, and D.J. Spry, *J. Appl. Phys.* 91, 6553 (2002).
20. A.V. Kuchuk, M. Guziewicz, R. Ratajczak, M. Wzorek, V.P. Kladko, and A. Piotrowska, *Mater. Sci. Eng. B* 165, 38 (2009).
21. A. Virshup, L.M. Porter, D. Lukco, K. Buchholt, L. Hultman, and A.L. Spetz, *J. Electron. Mater.* 38, 569 (2009).
22. M. Bhatnagar and B.J. Baliga, *IEEE Trans. Electron Devices* 40, 645 (1993).
23. S.-H. Ryu, S. Krishnaswami, M. O'Loughlin, J. Richmond, A. Agarwal, J. Palmour, and A.R. Hefner, *IEEE Trans. Dev. Lett.* 25, 556 (2004).
24. J.W. Palmour, S.T. Allen, R. Singh, L.A. Lipkin, and D.G. Waltz, *AIP Conf. Proc.* 361, 1321 (1996).
25. J. Crofton, L.M. Porter, and J.R. Williams, *Phys. Status Solidi B* 202, 581 (1997).
26. M. Green, *Solid State Surface Science* (New York: Marcel Dekker, 1969).
27. M. Melloch and J. Cooper Jr, *MRS Bull.* 22, 42 (1997).
28. E.H. Rhoderick, *IEE Proc.* 129, 1 (1982).
29. J. Andrews and M. Lepselter, *Solid-State Electron.* 13, 1011 (1970).
30. S.Y. Han, K.H. Kim, J.K. Kim, H.W. Jang, K.H. Lee, N.-K. Kim, E.D. Kim, and J.-L. Lee, *Appl. Phys. Lett.* 79, 1816 (2001).
31. J. Crofton, E.D. Luckowski, J.R. Williams, T. Isaacs-Smith, M.J. Bozack, and R. Siergiej, *Mater. Sci. Forum* 142, 569 (1996).
32. A. Itoh, T. Kimoto, and H. Matsunami, *IEEE Electron Device Lett.* 16, 280 (1995).
33. K. Vassilevski, K. Zekentes, K. Tsagaraki, G. Constantinidis, and I. Nikitina, *Mater. Sci. Eng. B* 80, 370 (2001).
34. F. Padovani and R. Stratton, *Solid State Electron.* 9, 695 (1966).
35. S. Cho, J. Lee, and H. Lee, *J. Appl. Phys.* 70, 282 (1991).
36. A. Yu, *Solid State Electron.* 13, 239 (1970).
37. C. Chang, Y. Fang, and S. Sze, *Solid-State Electron.* 14, 541 (1971).
38. N. Lundberg, *Solid-State Electron.* 38, 2023 (1995).
39. Y.-J. Lin, *Appl. Phys. Lett.* 86, 122109 (2005).
40. T. Nakamura and M. Satoh, *Solid-State Electron.* 46, 2063 (2002).
41. W. Schottky, *Naturwissenschaften* 26, 843 (1938).
42. N.F. Mott, *Proc. Camb. Philos. Soc.* 34, 568 (1938).
43. J. Bardeen, *Phys. Rev.* 71, 717 (1947).
44. A. Cowley and S. Sze, *J. Appl. Phys.* 36, 3212 (1965).
45. H. Tsuchida, I. Kamata, and K. Izumi, *J. Appl. Phys.* 85, 3569 (1999).
46. S.W. King, R.J. Nemanich, and R.F. Davisa, *J. Electrochem. Soc.* 146, 1910 (1999).
47. T. Teraji and S. Hara, *Phys. Rev. B* 70, 035312 (2004).
48. M. Losurdo, G. Bruno, A. Brown, and T.-H. Kim, *Appl. Phys. Lett.* 84, 4011 (2004).
49. J. Waldrop, R. Grant, Y. Wang, and R. Davis, *J. Appl. Phys.* 72, 4757 (1992).
50. F. Bozso, L. Muehlhoff, M. Trenary, W. Choyke, and J.T. Yates Jr, *J. Vac. Sci. Technol. A* 2, 1271 (1984).
51. S. Schoell, J. Howgate, M. Hoeb, M. Auernhammer, J. Garrido, M. Stutzmann, M. Brandt, and I. Sharp, *Appl. Phys. Lett.* 98, 182106 (2011).
52. N. Sieber, B. Mantel, T. Seyller, J. Ristein, L. Ley, T. Heller, D. Batchelor, and D. Schmeiber, *Appl. Phys. Lett.* 78, 1216 (2001).
53. N. Sieber, T. Seyller, L. Ley, D. James, J. Riley, R.C. Leckey, and M. Polcik, *Phys. Rev. B* 67, 205304 (2003).
54. H. Tsuchida, I. Kamata, and K. Izumi, *Appl. Phys. Lett.* 70, 3072 (1997).
55. M. Losurdo, M.M. Giangregorio, G. Bruno, A. Brown, and T.-H. Kim, *Appl. Phys. Lett.* 85, 4034 (2004).
56. L. Huang, Q. Zhu, M. Gao, F. Qin, and D. Wang, *Appl. Surf. Sci.* 257, 10172 (2011).
57. L. Huang, B. Liu, Q. Zhu, S. Chen, M. Gao, F. Qin, and D. Wang, *Appl. Phys. Lett.* 100, 263503 (2012).
58. B. Liu, L. Huang, Q. Zhu, F. Qin, and D. Wang, *Appl. Phys. Lett.* 104, 202101 (2014).
59. G.K. Reeves and H.B. Harrison, *IEEE Electron Device Lett.* EDL-3, 111 (1982).
60. G.K. Reeves, *Solid-State Electron.* 23, 487 (1980).
61. A. Addamiano, U.S. Patent No. 3,510,733 (1970).
62. S. Cichon, B. Barda, and P. Machac, *Radioengineering* 20, 209 (2011).
63. B. Barda, P. Machac, M. Hubickova, and J. Nahlik, *J. Mater. Sci.: Mater. Electron.* 19, 1039 (2008).
64. W.J. Lu, W.C. Mitchel, C.A. Thornton, G.R. Landis, and W.E. Collins, *J. Electron. Mater.* 32, 426 (2003).
65. E. Kurimoto, H. Harima, T. Toda, M. Sawada, M. Iwami, and S. Nakashima, *J. Appl. Phys.* 91, 10215 (2002).
66. B. Barda, P. Machac, and M. Hubickova, *Microelectron. Eng.* 85, 2022 (2008).
67. L.Q. Huang, Q.Z. Zhu, M.C. Gao, F.W. Qin, and D.J. Wang, *Jpn. J. Appl. Phys.* 51, 081302 (2012).
68. P. Machac, B. Barda, and M. Hubickova, *Microelectron. Eng.* 85, 2016 (2008).
69. P. Machac and B. Barda, *Proc. 32nd International Spring Seminar on Electronics Technology,* May 13–17, 2009, Brno, CZ, pp. 1–4.
70. S. Cichon, P. Machac, B. Barda, and M. Kudrnova, *Microelectron. Eng.* 106, 132 (2013).
71. P. Machac and B. Barda, *International Conference on Advanced Semiconductor Devices and Microsystems*, Oct. 12–16, 2008, Smolenice, SK, pp. 183–186.
72. C. Deeb and A.H. Heuer, *Appl. Phys. Lett.* 84, 1117 (2004).
73. W. Daves, A. Krauss, V. Haublein, A.J. Bauer, and L. Frey, *ECS J. Solid State Sci. Technol.* 1, P23 (2012).
74. K. Buchholt, R. Ghandi, M. Domeij, C.M. Zetterling, J. Lu, P. Eklund, L. Hultman, and A.L. Spetz, *Appl. Phys. Lett.* 98, 042108 (2011).
75. L.J. Evans, R.S. Okojie, and D. Lukco, *Mater. Sci. Forum* 717, 841 (2012).
76. H.S. Lee, M. Domeij, C.M. Zetterling, M. Östling, and J. Lu, *Mater. Sci. Forum* 527–529, 887 (2006).
77. A.V. Kuchuk, M. Guziewicz, R. Ratajczak, M. Wzorek, V.P. Kladko, and A. Piotrowska, *Microelectron. Eng.* 85, 2142 (2008).
78. L. Sang-Kwon, S. Eun-Kyung, C. Nam-Kyu, P. Hyo-Duck, L. Uneus, and A.L. Spetz, *Solid-State Electron.* 49, 1297 (2005).

79. P. Machac, B. Barda, and J. Maixner, *Appl. Surf. Sci.* 254, 1691 (2008).
80. H. Yang, T.H. Peng, W.J. Wang, D.F. Zhang, and X.L. Chen, *Appl. Surf. Sci.* 254, 527 (2007).
81. W. Lu, W.C. Mitchel, G.R. Landis, T.R. Crenshaw, and W.E. Collins, *J. Appl. Phys.* 93, 5397 (2003).
82. S. Tsukimoto, T. Sakai, T. Onishi, K. Ito, and M. Murakami, *J. Electron. Mater.* 34, 1310 (2005).
83. K. Ito, T. Onishi, H. Takeda, K. Kohama, S. Tsukimoto, M. Konno, Y. Suzuki, and M. Murakami, *J. Electron. Mater.* 37, 1674 (2008).
84. F.A. Mohammad, Y. Cao, and L.M. Porter, *J. Electron. Mater.* 36, 312 (2007).
85. K. Jung, Y. Sutou, and J. Koike, *Thin Solid Films* 520, 6922 (2012).
86. W. Daves, A. Krauss, V. Haublein, A.J. Bauer, and L. Frey, *J. Electron. Mater.* 40, 1990 (2011).
87. M. Vivona, G. Greco, F. Giannazzo, R. Lo Nigro, S. Rascunà, M. Saggio, and F. Roccaforte, *Semicond. Sci. Technol.* 29, 075018 (2014).
88. H. Yang, T.H. Peng, W.J. Wang, W.Y. Wang, and X.L. Chen, *Appl. Surf. Sci.* 255, 3121 (2008).
89. S. Cichon, P. Machac, B. Barda, V. Machovic, and P. Slepicka, *Thin Solid Films* 520, 4378 (2012).
90. G.Y. McDaniel, S.T. Fenstermaker, W.V. Lampert, and P.H. Holloway, *J. Appl. Phys.* 96, 5357 (2004).
91. J.O. Olowolafe, J.S. Solomon, W. Mitchel, and W.V. Lampert, *Thin Solid Films* 479, 59 (2005).
92. T.-Y. Zhou, X.-C. Liu, C.-C. Dai, W. Huang, S.-Y. Zhuo, and E.-W. Shi, *Mater. Sci. Eng. B* 188, 59 (2014).
93. A. Virshup, F. Liu, D. Lukco, K. Buchholt, A.L. Spetz, and L.M. Porter, *J. Electron. Mater.* 40, 400 (2011).
94. B. Barda, P. Machac, S. Cichon, V. Machovic, M. Kudrnova, A. Michalcova, and J. Siegel, *Appl. Surf. Sci.* 257, 414 (2010).
95. S. Liu, Z. He, L. Zheng, B. Liu, F. Zhang, L. Dong, L. Tian, Z. Shen, J. Wang, Y. Huang, Z. Fan, X. Liu, G. Yan, W. Zhao, L. Wang, G. Sun, F. Yang, and Y. Zeng, *Appl. Phys. Lett.* 105, 122106 (2014).
96. T. Ohyanagi, Y. Onose, and A. Watanabe, *J. Vac. Sci. Technol. B* 26, 1359 (2008).
97. P. Machac and B. Barda, *Microelectron. Eng.* 87, 2499 (2010).
98. M. Guziewicz, A. Piotrowska, E. Kaminska, K. Grasza, R. Diduszko, A. Stonert, A. Turos, M. Sochacki, and J. Szmidt, *Mater. Sci. Eng. B* 135, 289 (2006).
99. F. Roccaforte, F. La Via, V. Raineri, L. Calcagno, and P. Musumeci, *Appl. Surf. Sci.* 184, 295 (2001).
100. S.K. Lee, S.M. Koo, C.M. Zetterling, and M. Ostling, *J. Electron. Mater.* 31, 340 (2002).
101. T. Jang, L.M. Porter, G.W.M. Rutsch, and B. Odekirk, *Appl. Phys. Lett.* 75, 3956 (1999).
102. M. Grodzicki, P. Mazur, R. Wasielewski, and A. Ciszewski, *Opt. Appl.* 43, 91 (2013).
103. O.J. Guy, G. Pope, I. Blackwood, K.S. Teng, L. Chen, W.Y. Lee, S.P. Wilks, and P.A. Mawby, *Surf. Sci.* 573, 253 (2004).
104. W.J. Lu, W.C. Mitchel, G.R. Landis, T.R. Crenshaw, and W.E. Collins, *J. Vac. Sci. Technol. A* 21, 1510 (2003).
105. S. Hertel, D. Waldmann, J. Jobst, A. Albert, M. Albrecht, S. Reshanov, A. Schoner, M. Krieger, and H.B. Weber, *Nat. Commun.* 3, 1 (2012).
106. A.V. Adedeji, A.C. Ahyi, J.R. Williams, M.J. Bozack, S.E. Mohney, B. Liu, and J.D. Scofield, *Mater. Sci. Forum* 527, 879 (2006).
107. R. Kakanakov, L. Kassamakova-Kolaklieva, N. Hristeva, G. Lepoeva, and K. Zekentes, *Int. Conf. Microelectron.* 1, 205 (2002).
108. J. Sung-Jae, B. Sangwon, K. Sang-Cheol, and L. Jeong-Soo, *J. Electron. Mater.* 42, 2897 (2013).
109. H. Tamaso, S. Yamada, H. Kitabayashi, and T. Horii, *Mater. Sci. Forum* 778, 669 (2014).
110. W. Shui-Jinn, C. Shu-Cheng, U. Kai-Ming, and B.W. Liou, *Solid-State Electron.* 49, 1937 (2005).
111. T. Nakamura and M. Satoh, *Mater. Sci. Forum* 389, 889 (2002).
112. C. Nam-Ihn, J. Kyung-Hwa, and C. Yong, *Semicond. Sci. Technol.* 19, 306 (2004).
113. N.I. Cho, Y. Choi, and S.J. Noh, *Diamond Relat. Mater.* 13, 1154 (2004).
114. W.J. Lu, W.C. Mitchel, G.R. Landis, T.R. Crenshaw, and W.E. Collins, *Solid-State Electron.* 47, 2001 (2003).
115. S. Tanimoto and H. Oohashi, *Mater. Sci. Forum* 615, 561 (2009).
116. F. La Via, F. Roccaforte, A. Makhtari, V. Raineri, P. Musumeci, and L. Calcagno, *Microelectron. Eng.* 60, 269 (2002).
117. A. Makhtari, F. La Via, V. Raineri, L. Calcagno, and F. Frisina, *Microelectron. Eng.* 55, 375 (2001).
118. T. Seyller, K.V. Emtsev, F. Speck, K.Y. Gao, and L. Ley, *Appl. Phys. Lett.* 88, 242103 (2006).
119. J.W. Lee, B. Angadi, H.C. Park, D.H. Park, J.W. Choi, W.K. Choi, and T.W. Kim, *J. Electrochem. Soc.* 154, H849 (2007).
120. F. La Via, F. Roccaforte, V. Raineri, M. Mauceri, A. Ruggiero, P. Musumeci, L. Calcagno, A. Castaldini, and A. Cavallini, *Microelectron. Eng.* 70, 519 (2003).
121. S.Y. Han and J.L. Lee, *J. Electrochem. Soc.* 149, G189 (2002).
122. S.Y. Han, N.K. Kim, E.D. Kim, and J.L. Lee, *Mater. Sci. Forum* 389, 897 (2002).
123. M.W. Cole, P.C. Joshi, and M. Ervin, *J. Appl. Phys.* 89, 4413 (2001).
124. W. Huang, S.H. Chang, X.C. Liu, Z.Z. Li, T.Y. Zhou, Y.Q. Zheng, J.H. Yang, and E.W. Shi, *Mater. Sci. Forum* 740, 485 (2013).
125. H. Hanafusa, A. Ohta, R. Ashihara, K. Maruyama, T. Mizuno, S. Hayashi, H. Murakami, and S. Higashi, *Mater. Sci. Forum* 778, 649 (2014).
126. J.S. Shier, *J. Appl. Phys.* 41, 771 (1970).
127. J. Crofton, S.E. Mohney, J.R. Williams, and T. Isaacs-Smith, *Solid-State Electron.* 46, 109 (2002).
128. B. Pecz, L. Toth, M.A. di Forte-Poisson, and J. Vacas, *Appl. Surf. Sci.* 206, 8 (2003).
129. B.J. Johnson, *J. Appl. Phys.* 95, 5616 (2004).
130. B.P. Downey, S.E. Mohney, T.E. Clark, and J.R. Flemish, *Microelectron. Reliab.* 50, 1967 (2010).
131. A. Frazzetto, F. Giannazzo, R. Lo Nigro, V. Raineri, and F. Roccaforte. *J. Phys. D Appl. Phys.* 44, 255302 (2011).
132. R. Konishi, R. Yasukochi, O. Nakatsuka, Y. Koide, M. Moriyama, and M. Murakami, *Mater. Sci. Eng. B* 98, 286 (2003).
133. S. Tsukimoto, K. Nitta, T. Sakai, M. Moriyama, and M. Murakami, *J. Electron. Mater.* 33, 460 (2004).
134. K. Smedfors, L. Lanni, M. Ostling, and C.M. Zetterling, *Mater. Sci. Forum* 778, 681 (2014).
135. H. Vang, M. Lazar, P. Brosselard, C. Raynaud, P. Cremillieu, J.L. Leclercq, J.M. Bluet, S. Scharnholz, and D. Planson, *Superlattices Microstruct.* 40, 626 (2006).
136. M.R. Jennings, A. Perez-Tomas, M. Davies, D. Walker, L. Zhu, P. Losee, W. Huang, S. Balachandran, O.J. Guy, J.A. Covington, T.P. Chow, and P.A. Mawby, *Solid-State Electron.* 51, 797 (2007).
137. B. Krishnan, S.P. Kotamraju, G. Melnychuk, N. Merrett, and Y. Koshka, *Mater. Sci. Forum* 615, 581 (2009).
138. B.P. Downey, J.R. Flemish, B.Z. Liu, T.E. Clark, and S.E. Mohney, *J. Electron. Mater.* 38, 563 (2009).
139. S.H. Wang, O. Arnold, C.M. Eichfeld, S.E. Mohney, A.V. Adedeji, and J.R. Williams, *Mater. Sci. Forum* 527, 883 (2006).
140. S.K. Lee, C.M. Zetterling, E. Danielsson, M. Östling, J.P. Palmquist, H. Högberg, and U. Jansson, *Appl. Phys. Lett.* 77, 1478 (2000).
141. R. Kakanakov, L. Kassamakova, N. Hristeva, G. Lepoeva, N.I. Kuznetsov, and K. Zekentes, *Mater. Sci. Forum* 389, 917 (2002).
142. F.A. Mohammad, Y. Cao, K.C. Chang, and L.M. Porter, *Jpn. J. Appl. Phys.* 44, 5933 (2005).

143. L. Kolaklieva, R. Kakanakov, T. Marinova, and G. Lepoeva, *Mater. Sci. Forum* 483, 749 (2005).
144. B.H. Tsao, J. Lawson, and J.D. Scofield, *Mater. Sci. Forum* 527, 903 (2006).
145. K.H. Jung, N.I. Cho, J.H. Lee, S.J. Yang, C.K. Kim, B.T. Lee, K.H. Rim, N.K. Kim, and E.D. Kim, *Mater. Sci. Forum* 389, 913 (2002).
146. T. Jang, J.W. Erickson, and L.M. Porter, *J. Electron. Mater.* 31, 506 (2002).
147. T. Sakai, K. Nitta, S. Tsukimoto, M. Moriyama, and M. Murakami, *J. Appl. Phys.* 95, 2187 (2004).
148. R. Kakanakov, L. Kassamakova, I. Kassamakov, K. Zekentes, and N. Kuznetsov, *Mater. Sci. Eng. B* 80, 374 (2001).
149. T. Oder, J. Williams, M. Bozack, V. Iyer, S. Mohney, and J. Crofton, *J. Electron. Mater.* 27, 324 (1998).
150. C.M. Eichfeld, M.A. Horsey, S.E. Mohney, A.V. Adedeji, and J.R. Williams, *Thin Solid Films* 485, 207 (2005).
151. L. Kassamakova, R. Kakanakov, N. Nordell, S. Savage, A. Kakanakova-Georgieva, and T. Marinova, *Mater. Sci. Eng. B* 61, 291 (1999).
152. S. Liu and J. Scofield, HITEC (1998), pp. 88–92.
153. B.P. Downey, S.E. Mohney, and J.R. Flemish, *J. Electron. Mater.* 40, 406 (2011).
154. R. Kakanakov, L. Kasamakova-Kolaklieva, N. Hristeva, G. Lepoeva, J.B. Gomes, I. Avramova, and T. Marinova, *Mater. Sci. Forum* 457, 877 (2004).
155. M.R. Jennings, C.A. Fisher, D. Walker, A. Sanchez, A. Perez-Tomas, D.P. Hamilton, P.M. Gammon, S.E. Burrows, S.M. Thomas, Y. Sharma, F. Li, and P.A. Mawby, *Mater. Sci. Forum* 778, 693 (2014).
156. J. Crofton, P. McMullin, J. Williams, and M. Bozack, *J. Appl. Phys.* 77, 1317 (1995).
157. S. Tsukimoto, T. Sakai, and M. Murakami, *J. Appl. Phys.* 96, 4976 (2004).
158. B.H. Tsao, J. Lawson, and J. Scofield, *MRS Proc.* 911, 0911-B11-03 (2006).
159. S. Tsukimoto, K. Ito, Z.C. Wang, M. Saito, Y. Ikuhara, and M. Murakami, *Mater. Trans.* 50, 1071 (2009).
160. Z. Wang, S. Tsukimoto, M. Saito, and Y. Ikuhara, *Phys. Rev. B* 79 (2009).
161. M.R. Jennings, A. Perez-Tomas, D. Walker, L. Zhu, P. Losee, W. Huang, S. Balachandran, O.J. Guy, J.A. Covington, T.P. Chow, and P.A. Mawby, *Mater. Sci. Forum* 556, 697 (2007).
162. W. Lu, G.R. Landis, W.E. Collins, and W.C. Mitchel, *Mater. Sci. Forum* 527, 899 (2006).
163. J. Crofton, L. Beyer, J. Williams, E. Luckowski, S. Mohney, and J. Delucca, *Solid-State Electron.* 41, 1725 (1997).
164. S.E. Mohney, B.A. Hull, J.Y. Lin, and J. Crofton, *Solid-State Electron.* 46, 689 (2002).
165. B.J. Johnson and M.A. Capano, *Solid-State Electron.* 47, 1437 (2003).
166. J. Crofton, P.A. Barnes, J.R. Williams, and J.A. Edmond, *Appl. Phys. Lett.* 62, 384 (1993).
167. D.J. Spry and D. Lukco, *J. Electron. Mater.* 41, 915 (2012).
168. F. Laariedh, M. Lazar, P. Cremillieu, J. Penuelas, J.L. Leclercq, and D. Planson, *Semicond. Sci. Technol.* 28 (2013).
169. A. Baeri, V. Raineri, F. Roccaforte, F. La Via, and E. Zanetti, *Mater. Sci. Forum* 457, 873 (2004).
170. M.W. Cole, J.D. Demaree, C.W. Hubbard, M.C. Wood, and M.H. Ervin, i*n Proceedings of the 2004 IEEE Lester Eastman Conference on High Performance Devices*, vol. 65 (2002).
171. G.F. Eriksen and K. Dyrbye, *J. Micromech. Microeng.* 6, 55 (1996).
172. T. Marinova, A. Kakanakova-Georgieva, V. Krastev, R. Kakanakov, M. Neshev, L. Kassamakova, O. Noblanc, C. Arnodo, S. Cassette, and C. Brylinski, *Mater. Sci. Eng. B* 46, 223 (1997).
173. A. Baeri, V. Raineri, F. La Via, V. Puglisi, and G. Condorelli, *J. Vac. Sci. Technol. B* 22, 966 (2004).
174. F.A. Mohammad, Y. Cao, and L.M. Porter, *Appl. Phys. Lett.* 87, 161908 (2005).
175. M.H. Ervin, K.A. Jones, U. Lee, T. Das, and M.C. Wood, *Mater. Sci. Forum* 527, 859 (2006).
176. M.H. Ervin, K.A. Jones, U. Lee, and M.C. Wood, *J. Vac. Sci. Technol. B* 24, 1185 (2006).
177. S. Cichon, P. Machac, and J. Vojtik, *Mater. Sci. Forum* 740, 797 (2013).
178. N. Kiritani, M. Hoshi, S. Tanimoto, K. Adachi, S. Nishizawa, T. Yatsuo, H. Okushi, and K. Arai, *Mater. Sci. Forum* 433, 669 (2003).
179. L. Fursin, J.H. Zhao, and M. Weiner, *Electron. Lett.* 37, 1092 (2001).
180. R.S. Okojie, L.J. Evans, D. Lukco, and J.P. Morris, *IEEE Electron Device Lett.* 31, 791 (2010).
181. T. Kimoto, A. Itoh, H. Matsunami, T. Nakata, and M. Watanabe, *J. Electron. Mater.* 24, 235 (1995).
182. T. Kimoto, A. Itoh, H. Matsunami, T. Nakata, and M. Watanabe, *J. Electron. Mater.* 25, 879 (1996).
183. V. Heera, D. Panknin, and W. Skorupa, *Appl. Surf. Sci.* 184, 307 (2001).
184. H. Wirth, D. Panknin, W. Skorupa, and E. Niemann, *Appl. Phys. Lett.* 74, 979 (1999).
185. D. Panknin, H. Wirth, A. Mücklich, and W. Skorupa, *Mater. Sci. Eng. B* 61, 363 (1999).
186. J. Osterman, L. Abtin, U. Zimmermann, M. Janson, S. Anand, C. Hallin, and A. Hallén, *Mater. Sci. Eng. B* 102, 128 (2003).
187. M. Lazar, C. Raynaud, D. Planson, J.-P. Chante, M.-L. Locatelli, L. Ottaviani, and P. Godignon, *J. Appl. Phys.* 94, 2992 (2003).
188. A. Suchodolskis, A. Hallén, M.K. Linnarsson, J. Österman, and U.O. Karlsson, *Thin Solid Films* 515, 611 (2006).
189. M. Capano, S. Ryu, M. Melloch, J. Cooper Jr, and M. Buss, *J. Electron. Mater.* 27, 370 (1998).
190. M. Capano, S. Ryu, J. Cooper Jr, M. Melloch, K. Rottner, S. Karlsson, N. Nordell, A. Powell, and D. Walker Jr, *J. Electron. Mater.* 28, 214 (1999).
191. M.V. Rao, J.A. Gardner, P. Chi, O. Holland, G. Kelner, J. Kretchmer, and M. Ghezzo, *J. Appl. Phys.* 81, 6635 (1997).
192. S. Chou, Y. Chang, K. Weiner, T. Sigmon, and J. Parsons, *Appl. Phys. Lett.* 56, 530 (1990).
193. K. Jones, P. Shah, K. Kirchner, R. Lareau, M. Wood, M. Ervin, R. Vispute, R. Sharma, T. Venkatesan, and O. Holland, *Mater. Sci. Eng. B* 61, 281 (1999).
194. E.M. Handy, M.V. Rao, O. Holland, P. Chi, K. Jones, M. Derenge, R. Vispute, and T. Venkatesan, *J. Electron. Mater.* 29, 1340 (2000).
195. K. Mulpuri, S. Qadri, J. Grun, C. Manka, and M. Ridgway, *Solid-State Electron.* 50, 1035 (2006).
196. Y. Negoro, T. Kimoto, H. Matsunami, F. Schmid, and G. Pensl, *J. Appl. Phys.* 96, 4916 (2004).
197. K. Tone and J.H. Zhao, *IEEE Trans. Electron Devices* 46, 612 (1999).